PROCEEDINGS OF SCIENCE

Neutrino Structure Functions from GeV to EeV Energies

Alfonso Garcia-Soto[a,b,*]

[a] *Department of Physics & Laboratory for Particle Physics and Cosmology, Harvard University, Cambridge, MA 02138, USA*

[a] *Instituto de Física Corpuscular, CSIC-Universitat de València, 46980 Paterna, València, Spain.*

E-mail: alfonsogarciasoto@fas.harvard.edu,alfonso.garcia@ific.uv.es

Accurate theory calculations for neutrino-nucleus scattering rates are essential in interpreting neutrino experiments, from oscillation measurements to astroparticle physics at neutrino telescopes. In the deep-inelastic (DIS) regime, neutrino structure functions can be reliably evaluated in the framework of perturbative QCD. However, large uncertainties affect these structure functions at low momentum transfer, distorting event rate predictions for energies up to 1 TeV. We present a determination of the neutrino inelastic structure functions valid for all values of Q^2, from the resonance region to ultra-high energies. Our approach combines a data-driven machine learning parametrization of neutrino structure functions at low and moderate Q^2 values matched to perturbative QCD calculations at large Q^2. We compare our results to other calculations in the literature and outline the implications for neutrino telescopes.

38th International Cosmic Ray Conference (ICRC2023)
26 July - 3 August, 2023
Nagoya, Japan

*Speaker

PoS(ICRC2023)1208

1. Introduction

The double-differential cross section for neutrino-nucleus inelastic scattering can be decomposed in terms of structure functions as follows:

$$\frac{\mathrm{d}^2\sigma}{\mathrm{d}x\mathrm{d}y} = \frac{G_F^2 m_n E_\nu}{\pi(1+Q^2/m_W^2)^2}[(1-y)F_2(x,Q^2) + y^2 x F_1(x,Q^2) + y(1-\frac{y}{2})xF_3(x,Q^2)]$$

Where E_ν is the neutrino energy, m_n is the nucleon mass, x is Bjorken-x, Q is the momentum transfer, and y is the inelasticity ($= Q^2/(2m_N x E_\nu)$).

For momentum transfers above a few GeV, neutrino structure functions can be evaluated in perturbative QCD in terms of a factorized convolution of process-dependent partonic scattering cross sections and of process-independent parton distribution functions [1]. This scheme is used to make predictions of neutrino-nucleus scattering at high energies [2–6].

However, when the neutrino energy is $\sim$ 100 GeV, 20% of the inclusive cross section can arise from the $Q < 2$ GeV. Therefore, phenomenological models of low-Q structure functions have been developed to describe inelastic scattering at lower energies [7–12].

We present a new method, called NNSFν, to determine the neutrino-nucleon structure functions valid from low to high momentum transfers. The NNSFν predictions are extremely relevant for the current and next generation of neutrino telescopes [13–18] and for LHC far-forward neutrino scattering experiments [19–21].

2. The NNSFν method

In this section, we describe the overall strategy used to determine structure functions in NNSFν. Fig. 1 shows a schematic representation of the NNSFν method to compute neutrino structure functions. This strategy allows us to extend the perturbative QCD computations into the non-perturbative region. The different regions are described as follows:

- Region I: The perturbative calculation of neutrino structure functions is affected by significant theory uncertainties. Therefore, a neural network is trained using the information from the available experimental data.
- Region II: Structure functions are computed at NLO by `YADISM` [22] with nNNPDF3.0 [23] as input for all targets. In this region, the neural network parametrization is fitted to these QCD predictions rather than to the data as in Region I.
- Region III: The neural network predictions are replaced by the direct outcome of the same `YADISM` NLO calculation used to constrain the fit in Region II.

The parameterization of neutrino structure functions applicable in Regions I requires experimental data. We consider all available neutrino scattering data to be restricted to the inelastic regime. Apart from the Q_{dat} cut, we require the invariant mass of the final hadronic state to be larger than 2 GeV. In total, we have more than 4000 data points in the fit from different targets:

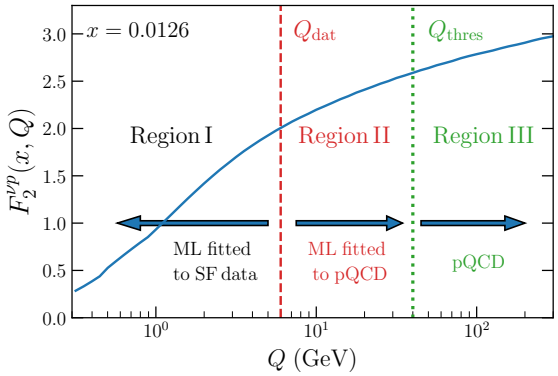

Figure 1: Schematic representation of the NNSFν strategy to parametrize neutrino structure functions.

Ne (BEBCWA59 [24]), Fe (CCFR [25], CDHSW [26], and NuTeV [27]), Pb (CHORUS [28]), and $CaCO_3$ (CHARM [29]). The measurements are presented in terms of either differential cross section or individual structure functions in (x, Q^2, A).

The NNSFν parameterization follows the NNPDF fitting methodology [30], based on the combination of neural networks as universal unbiased interpolator with the Monte Carlo replica method for error estimate and propagation. The network output includes a preprocessing factor that facilitates the learning and extrapolation of structure functions in the small-x region [31]. In addition, we subtract the behavior at $x = 1$ to reproduce the elastic limit where structure functions vanish due to kinematic constraints. Hyperparameters like the network architecture are determined by means of a dedicated optimization procedure.

The baseline fit shows a total of $\chi^2_{\rm exp} = 1.287$, and we do not observe outliers in the fits to data from single experiments. In addition, the fit quality is similar if the QCD structure function constraints are not included with a $\Delta\chi^2 = 0.1$.

3. Total cross section

The inclusive cross section is obtained by integrating over x and Q^2

$$\sigma^{\nu N}(E_\nu) = \int_{Q^2_{\rm min}}^{Q^2_{\rm max}} {\rm d}Q^2 \int_{x_0(Q^2)}^{1} {\rm d}x \frac{{\rm d}^2\sigma^{\nu N}}{{\rm d}x{\rm d}Q^2}(x, Q^2)$$

where the integration limits are given by

$$Q^2_{\rm max} = 2m_N E_\nu \qquad x_0(Q^2) = \frac{Q^2}{2m_N E_\nu}$$

The lower integration limit Q^2_{min} should go all the way down to zero. Previous studies impose a cut in Q^2_{min} to restrict the integration to the perturbative region. This is not required within the NNSFν approach since the structure functions are calculated for all Q^2 values. For the calculations presented in this section, a kinematic cut in the final-state invariant mass of $W > 2$ GeV is applied to restrict the calculation to the inelastic scattering region. The total uncertainty is evaluated using the uncertainty prescription for the structure-function grids.

Fig. 2 displays the inclusive (anti)neutrino-Oxygen inelastic cross section as a function of the neutrino energy E_ν. The NNSFν prediction is compared with the Bodek-Yang, BGR, and CSMS calculations. The NNSFν model is the only available prediction applicable in the complete range of E_ν relevant for neutrino telescopes. The region of applicability of the Bodek-Yang calculation is $E_\nu < 10^5$ GeV, while CSMS and BGR are restricted to $E_\nu > 100$ GeV. In the comparisons of Fig. 2, CSMS and BGR predictions are provided for a free isoscalar target and hence do not account for nuclear modification effects.

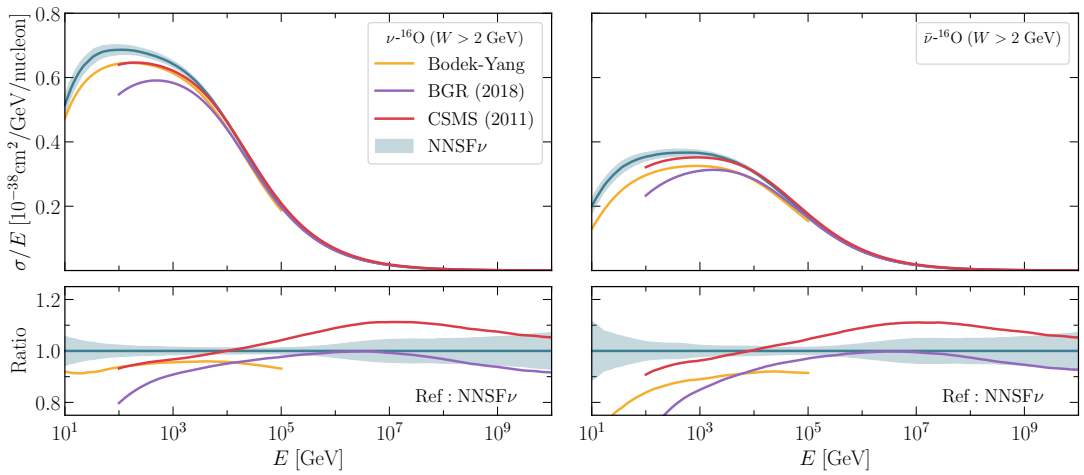

Figure 2: The inclusive neutrino (left) and antineutrino (right) inelastic cross section on Oxygen as a function of the neutrino energy. The NNSFν prediction and the associated 68% CL uncertainty are compared with the central values of the Bodek-Yang, BGR, and CSMS calculations.

NNSFν predicts a larger cross section than Bodek-Yang by a factor between 5% and 15%, depending on the E_ν value. In the high-energy region, the NNSFν prediction is bracketed by the CSMS above and BGR below. The differences with BGR are explained by combining the input PDFs and the treatment of top quark mass effects (NNSFν uses FFNS5, and BGR is based on FONLL).

Fig. 3 displays the NNSFν predictions for the inelastic cross section comparing the results of neutrino and antineutrino projectiles on oxygen, iron, and lead targets. Differences between inclusive cross sections on different targets are moderate for energies in the intermediate region between 10 TeV and a few PeV. In the high-energy region, the most marked effect is the strong suppression of the cross sections in lead compared to lighter targets, reaching up to 20% at 100 EeV. For neutrinos, differences remain at the few percent level in the region where the non-DIS contribution is sizable, whereas, for antineutrinos, a suppression is observed for heavier targets.

Two types of nuclear effects are responsible for differences between scattering rates on a heavy and light nucleus. The first is related to the different content of protons and neutrons. Compared to an isoscalar target, heavy nuclear targets display a different content of valence quarks which leads to a change in the associated structure functions. This effect is most relevant in the valence structure function region. As the energy increases, the cross section becomes dominated by small-x scattering involving sea quarks and gluons.

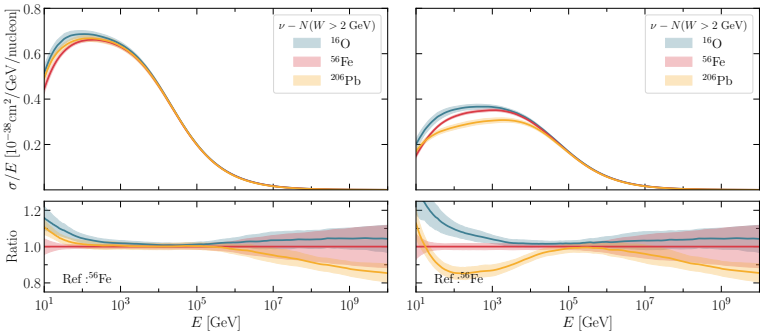

Figure 3: NNSFν prediction for the inclusive neutrino (left) and antineutrino (right) inelastic cross section on Oxygen, Iron, and Lead as a function of the neutrino energy. The bands represent the associated 68% CL uncertainty.

The second type of nuclear effect is modifying the bound nucleon's structure functions compared to free nucleon. In the perturbative QCD region, these modifications are encoded by the nuclear PDFs, here taken from the nNNPDF3.0 determination. The corrections, similar for neutrinos and antineutrinos, become most important in the shadowing region at medium and small-x, where a suppression in heavy nuclei is preferred. Given the large nPDF uncertainties, high-energy cross sections for heavy and light targets are compatible within errors.

Nuclear structure modification effects are also present for $E_\nu < 1$ TeV, a region where the low-Q contribution is significant and the factorization of nuclear PDFs does not work. Within the NNSFν framework, one estimates the nuclear modifications in that region by allowing a free dependence of $F_i(x, Q_2, A)$ to be directly constrained from the data and then matched to the QCD calculation at high-Q.

4. Inelasticity

The fraction of the incoming neutrino energy that is transferred to the hadronic final state is called inelasticity y. At $E_\nu < 100$ TeV, neutrino interactions are expected to produce, on average, more energetic hadronic showers than their antineutrino counterparts. Therefore, measuring the event-by-event inelasticity provides a useful proxy to separate ν and $\bar{\nu}$ interactions. This feature has already been exploited in IceCube analyses [32]. The mean value of the inelasticity as a function of the neutrino energy can be computed using as input a given prediction for the double-differential scattering cross section.

$$< y > (E_\nu) = \int_{Q^2_{\rm min}}^{Q^2_{\rm max}} {\rm d}Q^2 \int_{x_0(Q^2)}^{1} {\rm d}x\, y \frac{{\rm d}^2\sigma^{\nu N}}{{\rm d}x{\rm d}Q^2}(x, Q^2) \Big/ \sigma^{\nu N}(E_\nu)$$

Fig. 4 displays the mean value of the inelasticity as a function of the neutrino energy E_ν for both iron and lead targets. An overall good agreement is observed between the different predictions, with differences up to 10% depending on the target and E_ν ranges. Specifically, the NNSFν prediction is around 10% smaller than CSMS at high-neutrino energies. A good agreement between NNSFν and Bodek-Yang is found in the region of applicability of the latter.

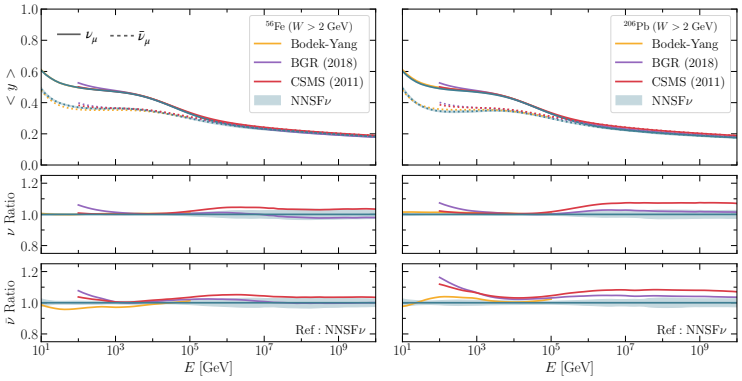

Figure 4: The mean inelasticity as a function of the neutrino energy E_ν for iron (left) and lead (right) targets. The NNSFν prediction, together with the associated 68% CL uncertainty band, is compared with the central values of the Bodek-Yang, BGR, and CSMS calculations.

5. Conclusions

We have presented a novel method to determine neutrino inelastic structure functions. The approach uses a data-driven parametrization at low values of Q^2 matched to perturbative QCD calculations at high Q^2. The resulting structure functions enable us to predict neutrino deep inelastic scattering from few GeV up to EeV energies and for different targets. In addition, the calculation includes uncertainties associated with the structure functions.

Comparisons with existing calculations in the literature show discrepancies in different energy regions mostly related to nuclear effects. Therefore, it is crucial to start accounting for these effects in analyses with neutrino telescopes for which systematic uncertainties are relevant.

The framework used to produce the NNSFν determination of neutrino inelastic structure functions can be obtained from the project website (https://nnpdf.github.io/nnusf). The structure functions are provided in `LHAPDF` grid format [33] and they have been tested with the HEDIS module of `GENIE` [34]. More details about this work can be found in [35].

Aknowlegments – A.G. acknowledges support from the European Union's H2020-MSCA Grant Agreement No. 101025085.

References

[1] J.M. Conrad, M.H. Shaevitz and T. Bolton, *Precision measurements with high-energy neutrino beams*, *Rev. Mod. Phys.* **70** (1998) 1341 [hep-ex/9707015].

[2] M. Gluck, P. Jimenez-Delgado and E. Reya, *On the charged current neutrino-nucleon total cross section at high energies*, *Phys. Rev.* **D81** (2010) 097501 [1003.3168].

[3] A. Connolly, R.S. Thorne and D. Waters, *Calculation of High Energy Neutrino-Nucleon Cross Sections and Uncertainties Using the MSTW Parton Distribution Functions and Implications for Future Experiments*, *Phys. Rev.* **D83** (2011) 113009 [1102.0691].

[4] A. Cooper-Sarkar, P. Mertsch and S. Sarkar, *The high energy neutrino cross-section in the Standard Model and its uncertainty*, *JHEP* **08** (2011) 042 [1106.3723].

[5] V. Bertone, R. Gauld and J. Rojo, *Neutrino Telescopes as QCD Microscopes*, *JHEP* **01** (2019) 217 [1808.02034].

[6] A. Garcia, R. Gauld, A. Heijboer and J. Rojo, *Complete predictions for high-energy neutrino propagation in matter*, *JCAP* **09** (2020) 025 [2004.04756].

[7] U.-K. Yang and A. Bodek, *Parton distributions, d/u, and higher twist effects at high x*, *Phys. Rev. Lett.* **82** (1999) 2467 [hep-ph/9809480].

[8] A. Bodek and U.K. Yang, *Modeling deep inelastic cross-sections in the few GeV region*, *Nucl. Phys. B Proc. Suppl.* **112** (2002) 70 [hep-ex/0203009].

[9] A. Bodek and U.K. Yang, *Modeling neutrino and electron scattering inelastic cross- sections in the few GeV region with effective LO PDFs TV Leading Order*, in *2nd International Workshop on Neutrino-Nucleus Interactions in the Few GeV Region*, 8, 2003 [hep-ex/0308007].

[10] A. Bodek, I. Park and U.-k. Yang, *Improved low Q**2 model for neutrino and electron nucleon cross sections in few GeV region*, *Nucl. Phys. B Proc. Suppl.* **139** (2005) 113 [hep-ph/0411202].

[11] A. Bodek and U.-k. Yang, *Axial and Vector Structure Functions for Electron- and Neutrino-Nucleon Scattering Cross Sections at all Q^2 using Effective Leading order Parton Distribution Functions*, 1011.6592.

[12] A. Bodek, U.K. Yang and Y. Xu, *Inelastic Axial and Vector Structure Functions for Lepton-Nucleon Scattering 2021 Update*, 2108.09240.

[13] IceCube collaboration, *Evidence for High-Energy Extraterrestrial Neutrinos at the IceCube Detector*, *Science* **342** (2013) 1242856 [1311.5238].

[14] KM3Net collaboration, *Letter of intent for KM3NeT 2.0*, *J. Phys. G* **43** (2016) 084001 [1601.07459].

[15] GRAND collaboration, *The Giant Radio Array for Neutrino Detection (GRAND): Science and Design*, *Sci. China Phys. Mech. Astron.* **63** (2020) 219501 [1810.09994].

[16] POEMMA collaboration, *The POEMMA (Probe of Extreme Multi-Messenger Astrophysics) observatory*, *JCAP* **06** (2021) 007 [2012.07945].

[17] KM3NeT collaboration, *Determining the neutrino mass ordering and oscillation parameters with KM3NeT/ORCA*, *Eur. Phys. J. C* **82** (2022) 26 [2103.09885].

[18] IceCube collaboration, *Determining neutrino oscillation parameters from atmospheric muon neutrino disappearance with three years of IceCube DeepCore data*, *Phys. Rev. D* **91** (2015) 072004 [1410.7227].

[19] J.L. Feng, I. Galon, F. Kling and S. Trojanowski, *ForwArd Search ExpeRiment at the LHC*, *Phys. Rev. D* **97** (2018) 035001 [1708.09389].

[20] SHiP collaboration, *SND@LHC*, 2002.08722.

[21] J.L. Feng et al., *The Forward Physics Facility at the High-Luminosity LHC*, 2203.05090.

[22] A. Candido, F. Hekhorn and G. Magni, *EKO: Evolution Kernel Operators*, 2202.02338.

[23] R. Abdul Khalek, R. Gauld, T. Giani, E.R. Nocera, T.R. Rabemananjara and J. Rojo, *nNNPDF3.0: evidence for a modified partonic structure in heavy nuclei*, *Eur. Phys. J. C* **82** (2022) 507 [2201.12363].

[24] BEBC WA59 collaboration, *Measurement of the Structure Functions F2 and Xf3 and Comparison With QCD Predictions Including Kinematical and Dynamical Higher Twist Effects*, *Z. Phys. C* **36** (1987) 1.

[25] E. Oltman et al., *Nucleon structure functions from high energy neutrino interactions*, *Z. Phys. C* **53** (1992) 51.

[26] J.P. Berge et al., *A Measurement of Differential Cross-Sections and Nucleon Structure Functions in Charged Current Neutrino Interactions on Iron*, *Z. Phys.* **C49** (1991) 187.

[27] NuTeV collaboration, *Precise measurement of neutrino and anti-neutrino differential cross sections*, *Phys. Rev. D* **74** (2006) 012008 [hep-ex/0509010].

[28] CHORUS collaboration, *Measurement of nucleon structure functions in neutrino scattering*, *Phys. Lett. B* **632** (2006) 65.

[29] CHARM collaboration, *Experimental Study of the Nucleon Structure Functions and of the Gluon Distribution from Charged Current Neutrino and anti-neutrinos Interactions*, *Phys. Lett. B* **123** (1983) 269.

[30] S. Forte, L. Garrido, J.I. Latorre and A. Piccione, *Neural network parametrization of deep inelastic structure functions*, *JHEP* **05** (2002) 062 [hep-ph/0204232].

[31] R.D. Ball, E.R. Nocera and J. Rojo, *The asymptotic behaviour of parton distributions at small and large x*, *Eur. Phys. J. C* **76** (2016) 383 [1604.00024].

[32] IceCube collaboration, *Measurements using the inelasticity distribution of multi-TeV neutrino interactions in IceCube*, *Phys. Rev. D* **99** (2019) 032004 [1808.07629].

[33] A. Buckley, J. Ferrando, S. Lloyd, K. Nordström, B. Page, M. Rüfenacht et al., *LHAPDF6: parton density access in the LHC precision era*, *Eur. Phys. J. C* **75** (2015) 132 [1412.7420].

[34] GENIE collaboration, *Recent highlights from GENIE v3*, *Eur. Phys. J. ST* **230** (2021) 4449 [2106.09381].

[35] A. Candido, A. Garcia, G. Magni, T. Rabemananjara, J. Rojo and R. Stegeman, *Neutrino Structure Functions from GeV to EeV Energies*, *JHEP* **05** (2023) 149 [2302.08527].